Additive Manufacturing of Cobalt-Based Dental Alloys: Analysis of Microstructure and Physico-Mechanical Properties

Leonhard Hitzler [a,b*#], Frank Alifui-Segbaya [c*#], Philipp Williams [d], Burkhard Heine [e], Michael Heitzmann [f], Wayne Hall [g], Markus Merkel [h], Andreas Öchsner [i]

[a] School of Engineering and Built Environment, Griffith University, Southport, Australia. Email: Leonhard.Hitzler@Griffithuni.edu.au

[b] Institute of Materials Science and Mechanics of Materials, Technical University of Munich, Garching, Germany. Email: Hitzler@wkm.mw.tum.de

[c] School of Dentistry and Oral Health, Griffith University, Southport, Australia. Email: f.alifui-segbaya@griffith.edu.au

[d] Faculty of Mechanical Engineering and Materials Science, Aalen University of Applied Sciences, Aalen, Germany. Email: Philipp.Williams@HS-Aalen.de

[e] Faculty of Mechanical Engineering and Materials Science, Aalen University of Applied Sciences, Aalen, Germany. Email: Burkhard.Heine@HS-Aalen.de

[f] School of Mechanical and Mining Engineering, The University of Queensland, Brisbane, Australia. Email: M.Heitzmann@UQ.edu.au

[g] School of Engineering and Built Environment, Griffith University, Southport, Australia. Email: W.Hall@Griffith.edu.au

[h] Faculty of Mechanical Engineering and Materials Science, Aalen University of Applied Sciences, Aalen, Germany. Email: Markus.Merkel@HS-Aalen.de

[i] Faculty of Mechanical Engineering, Esslingen University of Applied Sciences, Esslingen, Germany. Email: Andreas.Oechsner@HS-Esslingen.de

* First authors

 # Corresponding Authors: Hitzler@wkm.mw.tum.de; f.alifui-segbaya@griffith.edu.au

Declarations of interest: none.

Abstract

The limitations of investment casting of cobalt-based alloys are claimed to be less problematic with significant improvements in metal additive manufacturing by selective laser melting (SLM). Despite these advantages, the metallic devices are likely to display mechanical anisotropy in relation to build orientations, which could consequently affect their performance 'in vivo'. In addition, there are inconclusive evidence concerning the requisite composition and post-processing steps (e.g. heat-treatment to relieve stress) that must be completed prior to the devices being used. In the current paper, we evaluate the microstructure of ternary cobalt-chromium-molybdenum (Co-Cr-Mo) and cobalt-chromium-tungsten (Co-Cr-W) alloys built with Direct Metal Printing and LaserCUSING SLM systems respectively at 0°, 30°, 60° and 90° inclinations (Φ) in as-built (AB) and heat-treated (HT) conditions. The study also examines the tensile properties (Young's modulus, E; yield strength, $R_{P0.2}$; elongation at failure, A_t and ultimate tensile strength, R_m), relative density (RD), and micro-hardness (HV5) and macro-hardness (HV20) as relevant physico-mechanical properties of the alloys. Data obtained indicate improved tensile properties and HV values after short and cost-effective heat-treatment cycle of Co-Cr-Mo alloy; however, the process did not homogenize the microstructure of the alloy. Annealing heat-treatment of Co-Cr-W led to significant isotropic characteristics with increased E and A_t (except for $\Phi = 90°$) in contrast to decreased $R_{P0.2}$, R_m and HV values, compared to the AB form. Similarly, the interlaced weld-bead structures in AB Co-Cr-W were removed during heat-treatment, which led to a complete recrystallization in the microstructure. Both alloys exhibited defect-free microstructures with RD exceeding 99.5%.

Keywords

Cobalt-chromium alloy; Additive manufacturing; Selective laser melting; Microstructure; Tensile properties; Heat-treatment

1   Introduction

The high strength and stainless nature of ternary cobalt-chromium-molybdenum (Co-Cr-Mo) and cobalt-chromium-tungsten (Co-Cr-W) alloys, first patented in 1907 by Elwood Haynes, led to the development of compositional variants of cobalt-based alloys for clinical applications such as artificial knee and hip joints, and denture frameworks for fixed and removable prostheses [1]. In dentistry, the first use of a cobalt-based alloy for investment casting is reported to have started in 1936 [2]. This was a decade before William Taggart invented a practical method for casting gold inlays [3]. Although casting or 'lost-wax' technique is still popular in dental technology, the steps involved are time-consuming and fraught with processing variables. As such, the advent of selective laser melting (SLM) could indeed be considered a watershed as it is claimed to offer significant benefits in terms of manufacturing speed. Since the devices are digitally built, they are likely to produce predictable clinical outcomes and be much closer to manufacturers' specification [4-6]. SLM is a metal additive manufacturing (AM) process that employs high-energy laser beams to melt powders together, in a layer-by-layer fashion, into three-dimensional (3D) objects. However, it is a complex thermo-physical process, which is dependent on many parameters including alloying constituents, machines and the parameters of the controlled environment [6]. One of the potential limitations of the process is that, the devices are likely to display mechanical anisotropy in relation to build orientations and this could affect their performance 'in vivo' [7-10]. While a few studies [11, 12] have attempted to investigate this limitation, there are inconclusive evidence concerning requisite composition and post-processing steps (e.g. heat-treatment to relieve residual stress) [13] that must be completed prior to the devices being used. In the current paper, we evaluate the microstructure of commercially available ternary Co-Cr-Mo (ST2724G) and Co-Cr-W (Remanium CL) alloys, marketed for dental application. Samples were built with Direct Metal Printing and LaserCUSING SLM systems respectively at 0°, 30°, 60°and 90° inclinations to the layering (polar angle Φ) in 'as-built' (AB) and 'heat-treated'

(HT) forms. The study also evaluates the tensile properties (Young's modulus, E; yield strength, $R_{P0.2}$; elongation at failure, A_t and ultimate tensile strength, R_m), relative density (RD), and micro-hardness (HV5) and macro-hardness (HV20) as relevant physico-mechanical properties of the alloys

2   Experimental

2.1   Specimen preparation

AB and HT Co-Cr-Mo samples (Co Bal Cr 29 Mo 5.5 Si<1 Mn<1 Fe<1 wt.%) [14] were built with Type 5 ST2724G alloy (SINT-TECH Parc Européen d'Entreprises, Rue Richard Wagner 63200 Riom, France), whereas Co-Cr-W counterparts (Co Bal Cr 28 W 9 Si 1.5 Mn<1 Fe<1 Nb<1N<1 wt.%) [15] were built with Remanium star CL alloy (Dentaurum GmbH & Co. KG, Turnstraße 31, 75228 Ispringen, Germany) at 0°, 30°, 60° and 90° inclinations, subsequently referred to as polar angle (F). The ST2724G raw powder had a powder density of 4.1 g/cm^3 and an average particle size (D_{50}) of 8-9 µm. **Figure 1** shows the schematic of sample orientations. For Co-Cr-Mo specimens, a dumbbell-shaped CAD model (SolidWorks, Dassault Systèmes SolidWorks Corp., 300 Baker Avenue, Concord, MA 01742) designed in accordance with ISO 22674 requirements [16] was sent to 3D Systems (Rue Richard Wagner, 63200 Riom, France) and samples were built at layer thickness of 30 µm in an inert environment using ProX 200 DMP printer [17]. The heat treatment for Co-Cr-Mo was completed in an airy furnace at 800°C for 20 minutes by the manufacturer prior to the removal of the support structures (Mark Barnes Engineering, 35 Olympic Circuit, Southport QLD 4215, Australia) and is the recommended heat treatment stated by 3D Systems for this alloy in the scope of dental applications. Unlike the directly built Co-Cr-Mo specimens, Co-Cr-W specimens were supplied as 7 mm x 55 mm cylindrical bars built in an inert environment using a Mlab printer (Concept Laser GmbH, An der Zeil 8, 96215 Lichtenfels, Germany). Heat-treatment was completed by the supplier in a furnace under argon atmosphere at a rate of 400°C/hour to 1150°C followed by a 1 h dwell time

before cooling down to 300°C [18]. This particular treatment is recommended by Concept Laser for the Co-Cr-W alloy for dental applications. The cylindrical samples were turned on a CNC milling machine (Griffith Technical Solutions, Nathan Campus, Griffith University, 170 Kessels Road QLD 4111, Australia) using cooling emulsion to minimize possible alterations to their microstructure.
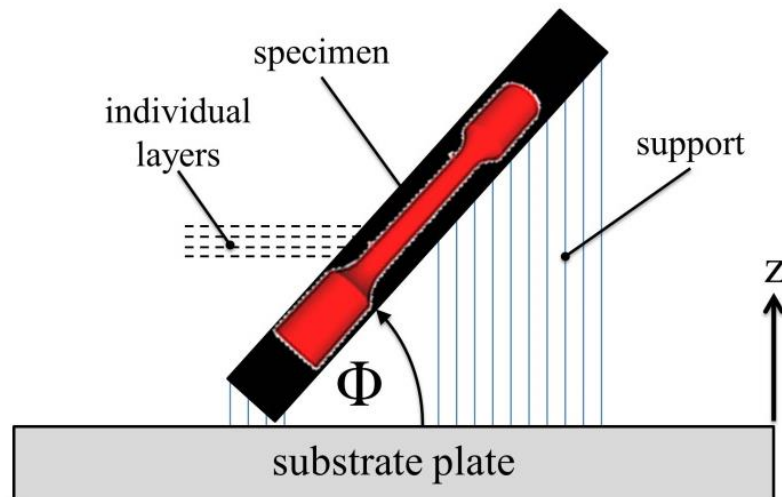

Figure 1. Schematic of sample orientations and description via the polar angle (F); $F = 0°$ equals sample orientation parallel to the layers; and $F = 90°$ a perpendicular alignment.

2.2   Microstructural analysis

The microstructure analysis involved optical examination of randomly selected test specimens for grain size, porosity and voids, dendritic growth, cracks and other defects. Four grinding and mechanical polishing steps were performed to expose the metallurgical structure. The steps comprised grinding with silicon carbide (SiC) 220 sandpaper, polishing process with 9 µm, 3 µm diamond suspension and surface finishing with a silicon monoxide (SiO) solution with a grain size of 0.5 µm. The visibility of the scan track pattern and the inherent grain structure was enhanced by a subsequent etching process. Two etching procedures were employed; these were etching with 'Berahra 3' acid (comprising 60 ml H_20, 40 ml hydrochloric acid, 5 g ammonium hydrogen difluoride, and 1 g potassium bisulphite) and electrochemical etching at 3 V for 10 seconds in a 3% hydrochloric acid solution. High-resolution images of the etched micro-

sections were taken with an optical light microscope (Axio Imager z2m, Carl Zeiss Microscopy GmbH, Jena, Germany). In determining the RD**,** area-porosities were calculated on the micrographs with the Zeiss AxioVison software package (Carl Zeiss Microscopy GmbH, Jena, Germany).

2.3   Tensile test

Tensile testing to assess Young's modulus (E), 0.2% yield strength ($R_{P0.2}$), elongation at failure (A_t) and ultimate tensile strength (R_m) was performed as per ISO 22674:2016 test guidelines [19] on test specimens ($n \geq 3$) from each configuration and condition (inclination and treatment) by subjecting them to uniaxial tensile loading until failure. Specimens (gauge diameter 3 mm, gauge length 15 mm, radial shoulders) were tested to yield at maximum load of 10 kN and 1.5 mm/min cross-head speed using an Instron 5584 tensile testing machine with an inbuilt video extensometer type 2663-821 (Instron Corp., Norwood, MA, USA). Applied nomenclature for the tensile properties are in accordance with DIN EN ISO 6892-1:2009 [20].

2.4   Hardness test

Vickers hardness (HV) tests were perfomed with a Struers Durascan 70 G5 hardness tester (Struers GmbH, Kernen im Remstal, Germany) in accordance with DIN EN ISO 6507-2:2016 test guidelines [21] to measure the micro-hardness (HV5) and macro-hardness (HV20) of the alloys. For HV5 the indentation force was 49.03 N and for HV20 196.1 N respectively.

3   Results

For microstructure analysis, only images from cross-sectional micrographs are presented in the paper due to the configurational similarities and corresponding redundancy of longitudinal micrographs **(Fig. 2)**. For instance, the cross-sectional cut of a 0° orientated specimen matches the longitudinal cut of a 90° specimen; likewise, the cross-sectional cut of a 30° inclined specimen matches the longitudinal cut of a 60° specimen. **Figure 3** shows the obtained area-

porosities of both alloys, measured on the micro-sections. The relative density (RD) is 99.93%
for Co-Cr-Mo and 99.86% for Co-Cr-W respectively. On a side note, relative densities obtained
via micro-sections results generally in higher percentages compared to the determination via
the Archimedes method [22]. On the 90° inclined Co-Cr-W sample was a small delamination
evident, which resulted in the spike in area-porosity. In **Figures 4** and **5** the microstructures of
Co-Cr-Mo and Co-Cr-W specimens are depicted for each inclination and both conditions, i.e.
as-fabricated and heat-treated, whereby the left columns refer to the as-built condition and the
right columns to the heat treated condition. The evaluated tensile properties are summarized in
Table 1 and exemplary stress strain diagrams are provided in **Figure 6**. **Figure 7** compares the
Young's modulus (E) data and summarizes its evolution after heat treatment and its dependency
on the inclination angle. Similarly, **Figure 8** presents the graphical summaries of the yield
strength ($R_{P0.2}$), elongation at failure (A_t) and ultimate tensile strength (R_m). In addition, the
corresponding minimum requirements stated in the ISO 22674 standard [16] are included in the
graphical summaries as well. Lastly, micro [HV5] and macro [HV20] hardness results are
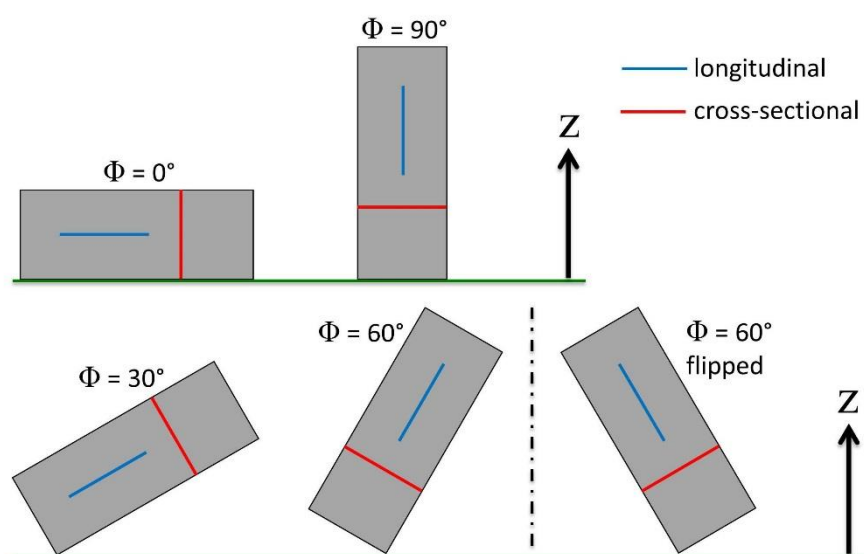summarized in **Figure 9.**

Figure 2. Configurational similarities in longitudinal and cross-sectional test samples.
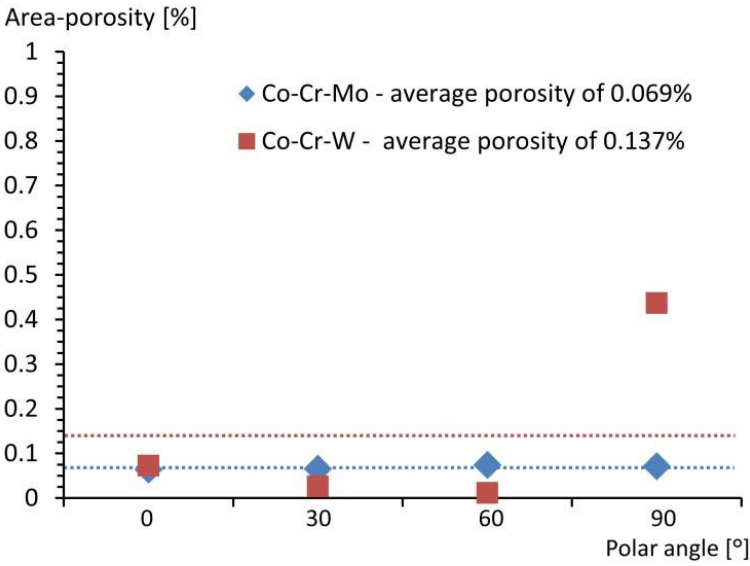
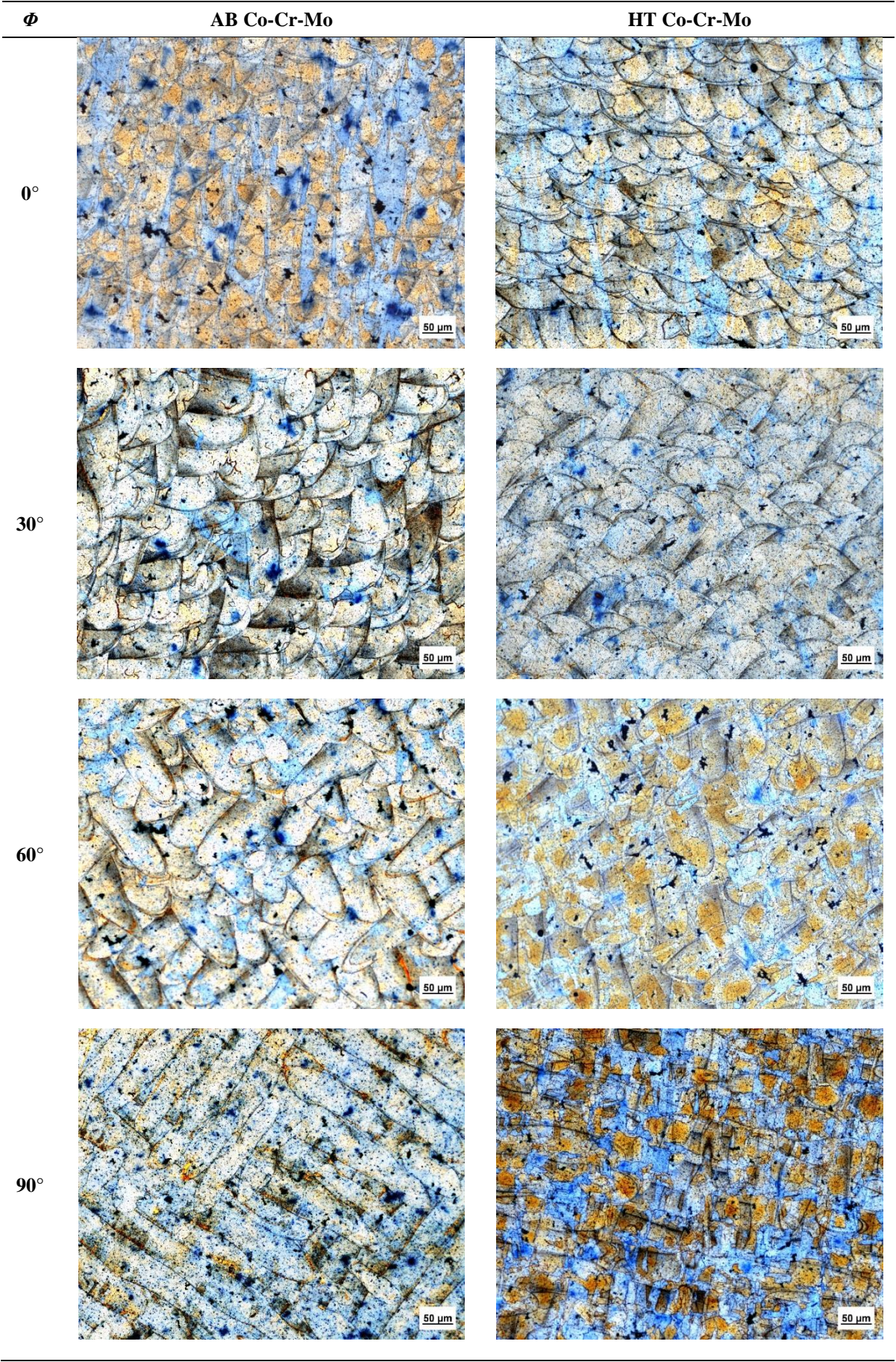**Figure 3.** Area porosity of the alloys per configuration

Φ	AB Co-Cr-Mo	HT Co-Cr-Mo
0°		
30°		
60°		
90°		

Figure 4. Microstructure (50 µm) of AB and HT Co-Cr-Mo specimens

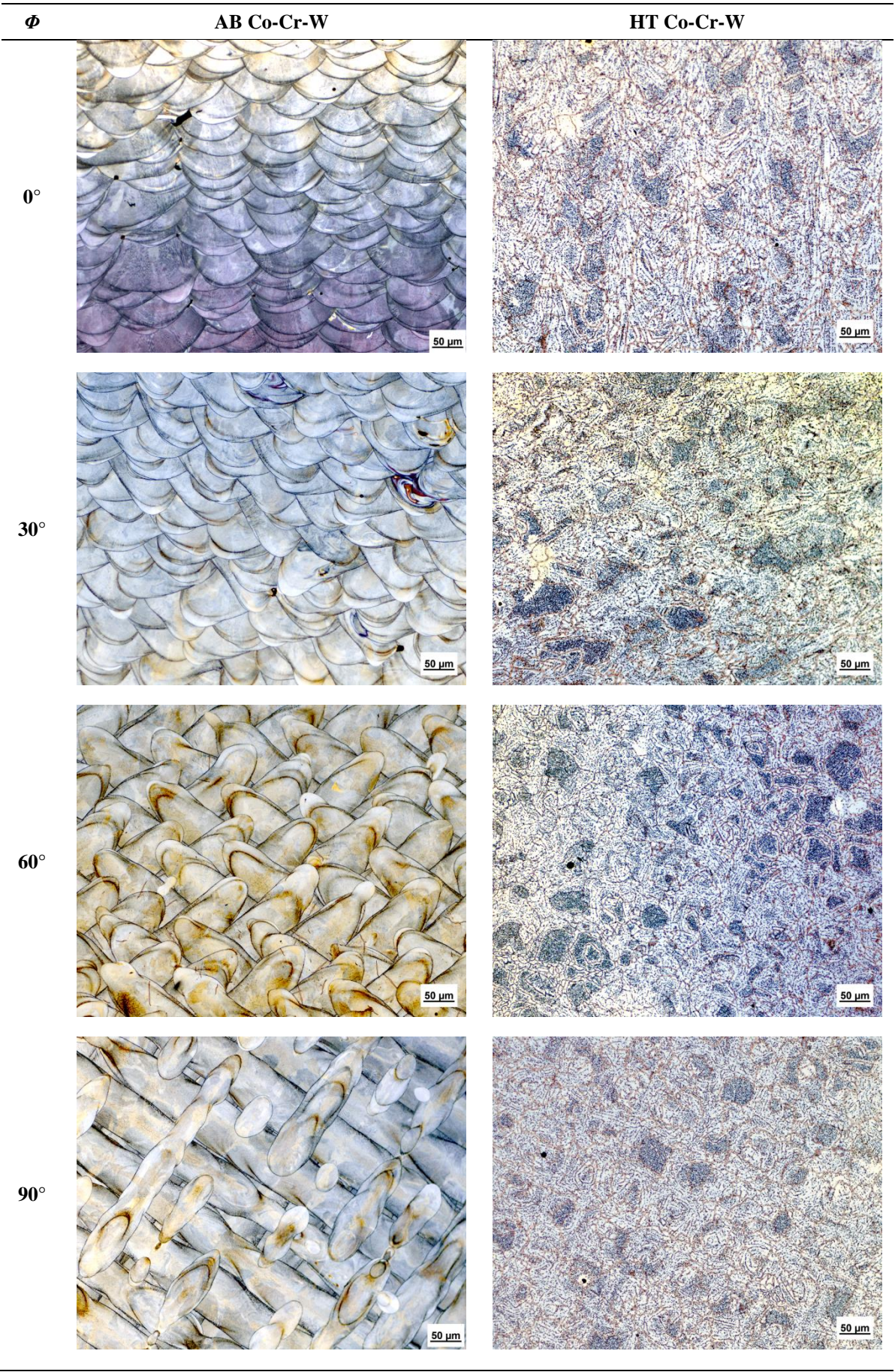| *Φ*	AB Co-Cr-W	HT Co-Cr-W
0°		
30°		
60°		
90°		

Figure 5. Microstructure (50 µm) of AB and HT Co-Cr-W specimens

Table 1. Tensile properties of Co-Cr-Mo and Co-Cr-W

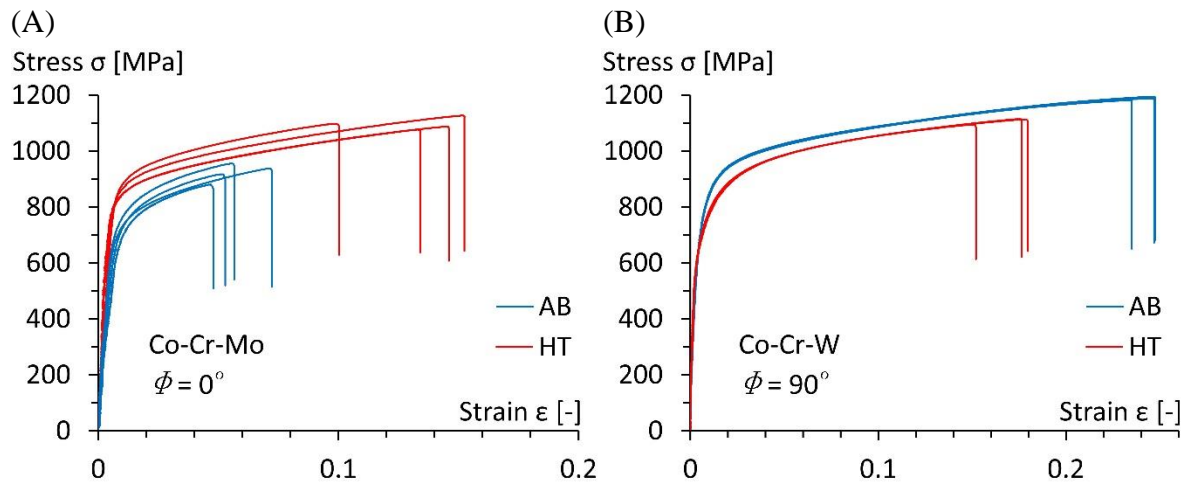| Alloy, condition and inclination (Φ)	Young's modulus E [GPa]		Yield strength $R_{P0.2}$ [MPa]		Elongation at failure A_t [%]		Ultimate tensile strength R_m [MPa]	
	Mean	STDEV	Mean	STDEV	Mean	STDEV	Mean	STDEV
Co-Cr-Mo 0°_AB	98.38	17.01	702	15.4	5.7	1.04	923	32.4
Co-Cr-Mo 0°_HT	156.48	19.50	819	29.1	13.3	2.32	1097	21.6
Co-Cr-Mo 30°_AB	105.32	19.39	783	23.7	6.7	1.94	1102	45.2
Co-Cr-Mo 30°_HT	149.73	6.29	1002	41.1	8.3	0.81	1262	14.1
Co-Cr-Mo 60°_AB	112.11	58.51	696	34.3	7.5	2.10	1012	24.0
Co-Cr-Mo 60°_HT	105.67	13.18	808	37.8	9.4	1.32	1054	20.9
Co-Cr-Mo 90°_AB	100.21	6.95	674	9.0	14.8	1.62	1033	12.4
Co-Cr-Mo 90°_HT	164.54	15.10	757	7.2	16.7	1.51	1052	6.3
Co-Cr-W 0°_AB	183.44	15.58	917	9.9	11.1	1.14	1263	8.6
Co-Cr-W 0°_HT	216.32	21.99	655	26.6	15.0	1.54	1111	8.9
Co-Cr-W 30°_AB	147.50	20.57	965	5.9	10.4	1.31	1272	10.3
Co-Cr-W 30°_HT	186.96	7.90	651	4.9	15.5	1.04	1127	12.3
Co-Cr-W 60°_AB	167.17	26.23	845	11.1	17.1	1.35	1247	6.1
Co-Cr-W 60°_HT	214.51	29.25	669	20.0	18.0	2.90	1162	13.4
Co-Cr-W 90°_AB	138.55	6.93	755	8.7	24.3	0.70	1188	6.3
Co-Cr-W 90°_HT	202.35	22.08	658	7.1	16.9	1.51	1108	10.9

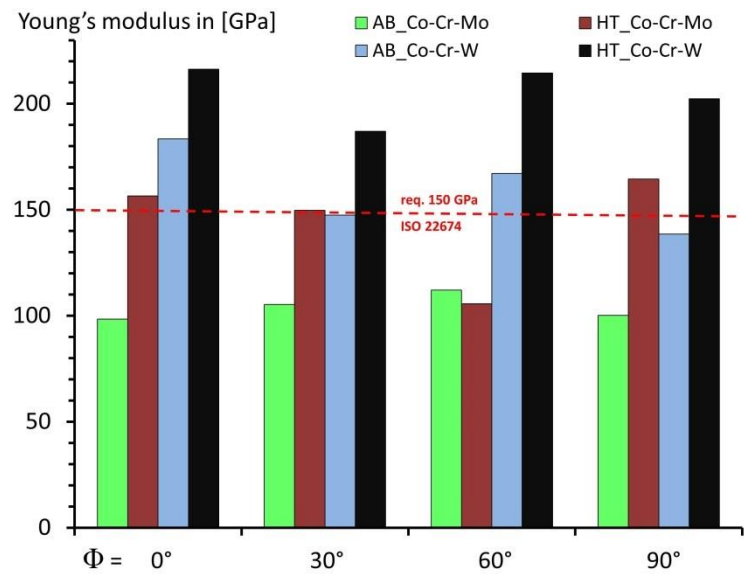**Figure 6.** Exemplary stress strain curves for (A) Co-Cr-Mo and (B) Co-Cr-W

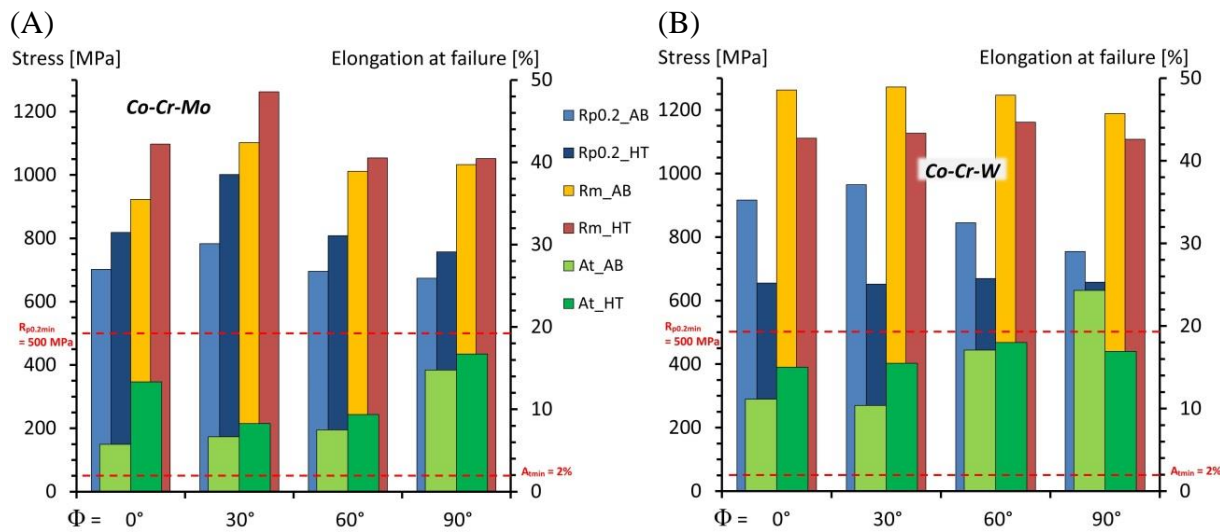**Figure 7.** Mean value of *E* for Co-Cr-Mo and Co-Cr-W alloys

Figure 8. Mean values of $R_{P0.2}$, A_t and R_m for Co-Cr-Mo (A) and Co-Cr-W (B) alloys
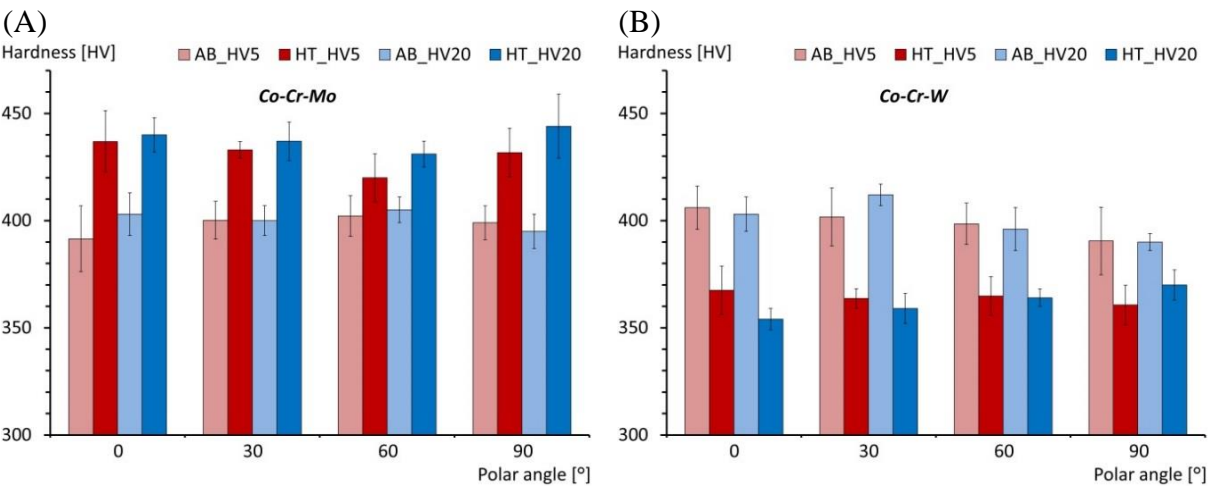
Figure 9. Mean values of HV5 and HV20 for Co-Cr-Mo (A) and Co-Cr-W (B) alloys.

4   Discussion

While in the mouth, dental devices are subjected to stress from masticatory actions, hence alloys should show high recovery capacity, resilience, high specific stiffness (E / RD) and elongation, if devices are to withstand biting forces without fracture [23]. **Figure 10** shows an illustration of a denture framework with different functional parts, such as clasp components and connectors. These parts explain the importance of orientation dependent fluctuations in the material characteristics, which are present in selective laser melted metal.

The standards for assessing the mechanical properties of dental alloys [19] place emphasis on E, A_t and $R_{P0.2}$ of the alloys. In a clinical context, $R_{P0.2}$ is relevant for predicting failure in multiple unit dental bridges. A_t determines how the alloys can sustain a large permanent deformation before they fracture. It is worth noting that, A_t could serve as a quality control measure that verifies the level of impurities and proper processing of the devices. While E measures the alloy's ability to resist flexure, especially in metal-ceramic restorations where any flexure will cause fracture of the porcelain [24]. Literature accompanying alloys provide information on their hardness; while a low value cannot resist occlusal forces, an extremely high could make the alloy difficult to grind and polish, and even wear the opposing teeth [23]. **Table 2** summarizes the tensile properties as a range, i.e. respective minima and maxima for alloys examined in comparison to data form alloy manufacturers and standard requirements for dental alloys.
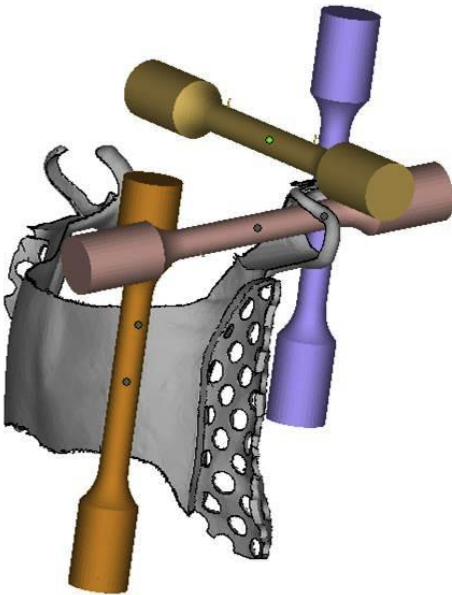
Figure 10. Schematic of a denture framework with different functional parts

Table 2. Tensile properties of alloys in comparison to standards requirements

	Young's modulus E [GPa]	Yield strength $R_{P0.2}$ [MPa]	Elongation at failure A_t [%]	Ultimate tensile strength R_m [MPa]	Additional information
AB Co-Cr-Mo range at 0º, 30º, 60º and 90º in current study	98.38 - 112.11	674 - 783	5.7 - 14.8	923 – 1102	Recommended heat treatment for dental parts is 800°C for 20-25 min.
HT Co-Cr-Mo range at 0º, 30º, 60º and 90º in current study	105.67 - 164.54	757[c] -1002	8.3 - 16.7	1012 – 1262	
AB Co-Cr-Mo data from manufacturer as per ASTM E8 [25]	**	850±100	10±2	1200±100	** Not provided Manufacturer density is ≈100% in AB and HT conditions; HV5after heat-treatment is 500±20
HT Co-Cr-Mo data from manufacturer as per ASTM E8 [25]	**	900±100	15±2	1260±100	
AB Co-Cr-W range at 0º, 30º, 60º and 90º in current study	138.55 - 183.44	755 - 965	10.4 - 24.3	1188 - 1263	Recommended heat treatment for dental parts is slow heating (400°C/h) up to 1150°C, followed by a dwell time of 1 h, then furnace cooling to 300°C
HT Co-Cr-W range at 0º, 30º, 60º and 90º in current study	186.96 - 216.32	651 – 669	15 -18	1108-1162	
HT Co-Cr-W data range (0º, 45º and 90º) from manufacturer [15]	230	792 - 835	8 - 11	1136 - 1200	Manufacturer density at all orientations is 8.6 g/cm^3
ISO 22674:2016 [16]	150	500	2	**	** Not provided

4.1   Microstructural analysis

SLM-produced Co-Cr alloys are reported to display superior homogeneity compared to cast Co-Cr alloys, which are inherently associated with large initial grain size, non-homogeneities and other casting defects [6].

4.1.1   Relative Density

The evaluated area-porosities on the micrographs revealed averaged RDs greater 99.8% and individual RDs greater than 99.5% in all cases. Since the applied heat-treatment in this study did not comprise a hot isostatic pressing (HIP), which could enhance further the RD, it can be concluded that the post heat treatment did not alter the RD of the specimens [26]. It is worth stating that, the observed density does not negate a possible inhomogeneity at increasing build height [9]. Given that the high quality criterion applied in the aeronautics industry is RD greater than 99%, these values could be considered to be exceptional for the manufacturing process [27]. For most applications, such a high RD is not required and a correlated reduction in mechanical strength is traded for speed and economic fabrication [28-30]. However, for dental metallic devices, the RD is also relevant to accomplish a tissue-friendly, void-free, satin finish, which is achieved via electrolytic polishing to prevent fitting, and cleaning problems on the fitting surface of denture frameworks. Given that in SLM the residual porosity tends to be common in the subsurface, which is the transition area between the contour and core irradiation, lower RD could potentially lead to laid open pores after polishing [10, 31, 32].

4.1.2   As-built condition

In the AB condition, the stacking scheme of the individual weld beads, as well as the applied irradiation strategy controls the micrographs (left-hand side on Figures 4 and 5). Noteworthy is the absence of needle-like appearing fine structured platelets, seen in cast samples, which are formed at thermodynamic equilibrium conditions at 417°C alongside the allotropic transformation from face centered cubic (fcc; γ–Co) to hexagonal close packed (hcp; ε–Co)

crystal structure [33]. In investment casting cooling rates are very slow within the pool of molten ingots, larger grains are formed around tiny nuclei that grow until the grain boundaries meet in the solid state. Because of this, dendritic structures may be very large in cast Co-Cr alloys, and the size of a single grain can approach the diameter of a removable partial denture framework clasp [5]. Due to the rapid cooling rates in SLM no large grains or dendritic structures are evident. Moreover, the absence of the platelets indicates that the fcc to hcp transformation did not take place and the thermodynamic equilibrium was not reached. This suggest that the metastable γ–Co is present in the as-built condition, which coincides with a recently published study on heat-treatments of additively manufactured Co-Cr-Mo. According to Kajima et al. [34] ε–Co is only present after an additional heat treatment and the volume fraction between γ–Co and ε–Co varies upon the heat treatment temperature, with γ–Co remaining as the predominant phase (≥ 75% volume fraction). The transformation of γ-Co to ε–Co is dependent on the grain size, and for fine grained structures, as is the case in SLM, this transformation is suppressed, resulting in the predominant γ–Co [35].

4.1.3 Heat treated condition

Heat treatments and modification of elemental composition could change the microstructure and consequently alter the physical-mechanical-chemical properties of Co-based alloys. In SLM, heat treatment is required to remove accumulated thermal stresses in long-span devices [13]. It is worth clarifying that the cycles for both alloys differ significantly. Co-Cr-Mo was HT at 800°C, which induced slow-progressing recrystallization whereas at 1150°C for Co-Cr-W, a soft annealing with directional recrystallization occurred. The latter led to a complete restructuration of the microstructure, whereby the stacking scheme of single weld beads was no more visible (Figure 5). At 1150 °C, Cr and W are solved in γ-Co and a chemically homogenous situation is given. This step was followed by a very slow cooling (furnace cooling), which ensured thermodynamic equilibrium conditions. Generally, the Co-Cr-W

material displayed predominantly isotropic properties with only minor fluctuations after heat-treatment; while E was raised significantly, strength and hardness were reduced. Savage [36] explained that the preferred temperature range for the isothermal transformation (notably by lamellar constituent) of the ternary Co-based alloys is about 1040°C to 1100°C and the length of the isothermal treatment is a function of composition of alloy and temperature of transformation, but in most instances one hour at temperature is sufficient. The isothermal heat-treatment at 800°C for 20 minutes of Co-Cr-Mo resulted in significantly improved E and slightly increased $R_{P0.2}$ A_t, R_m and HV. An assumption of the origin of the higher and unsystematically varied R_m was given in a study by Turrubiates-Estrada et al [37]. It was indicated that heat-treatment at 800°C for 20 minutes promotes the formation of ε–Co and intermetallic precipitations and/or carbides (**Fig. 11**, adapted from [38]). According to Kajima et al. [34] heat treatment at 800°C for 6 h can lead to a volume fraction of around 20-25% ε–Co in SLM samples. The formation of the second phases in a sufficient fine distribution (high undercooling) could be the origin of the observed raising of the mechanical values.
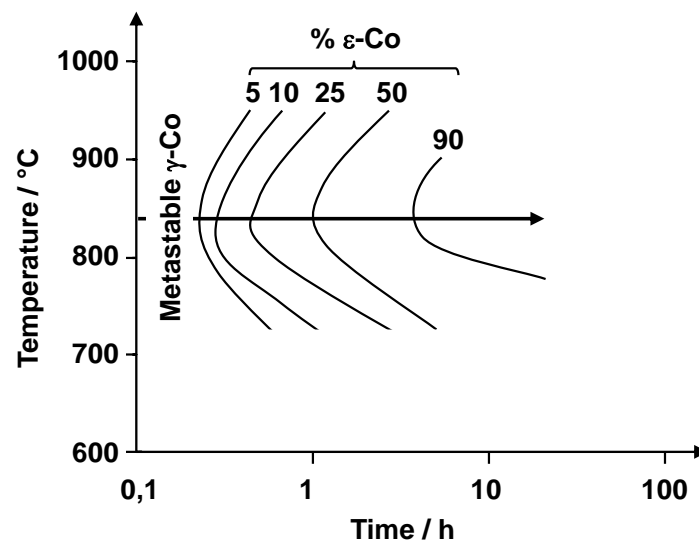

Figure 11. Isothermal TTT-diagram of CoCr27Mo5C0.23, adapted from [38]

It should be noted that during the additive forming the material undergoes several heating cycles. After the main fabrication step, i.e. the raw metal powder being completely molten and

rapidly solidified, the solidified volume passes a continuous time-temperature-transformation (TTT) as shown in **Figure 12**, adapted from [38]. During cooling the observed volume undergoes several post-heating by additive forming of further layers on top of the observed volume, hence, it is possible that a considerable fraction of ε–Co can be generated via alterations on the process conduct [10].
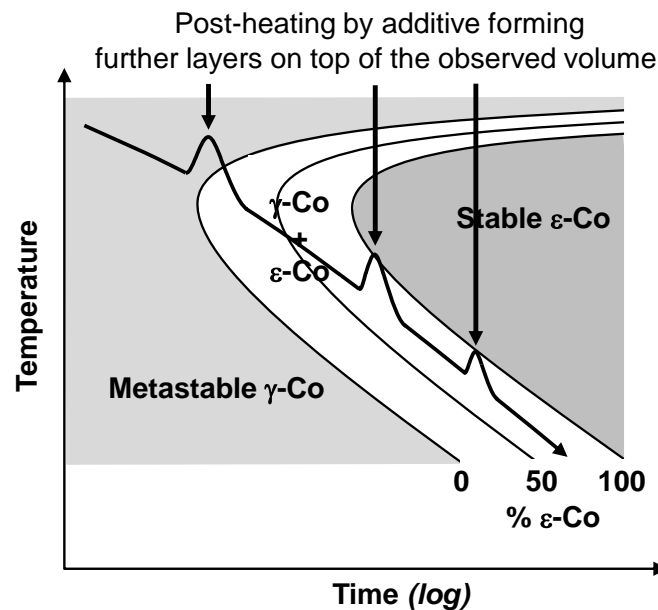

Figure 12. Continuous TTT-diagram schematically, adapted from [38]

4.2   Tensile properties

All test specimens yielded at the ultimate stress without localized necking. Specimen fracture occurred along the gauge length, indicating the homogeneous nature of the alloys. The overall polar angle dependence of the mechanical properties was low, except for A_t, which showed large fluctuations in the AB condition for both alloys, and for Co-Cr-Mo in the heat-treatment condition. These findings confirm the assertion that ductility represents the most volatile tensile characteristic. Our data for polar dependency at $\Phi = 90°$ corroborates findings by Takaichi et al. [12], but contrast studies that examine Al-based [9] and Fe-based [8] metals. This shows that in SLM characteristics on the anisotropy vary and are dependent on raw materials.

Although there is no existing manufacturer data on build orientations for Co-Cr- Mo alloy used in our study, our data show that Co-Cr-Mo in AB form required heat-treatment to attain the minimum E value as per standards requirements (except for $\Phi = 60°$). Despite the improved tensile properties and HV values, the short and cost-effective heat treatment cycle did not completely homogenize the properties of alloy. Both alloys showed increased E after heat-treatment, which is related to the increased ratio of ε–Co. Differences in E values for the two alloys are probably due to varying ratios of γ–Co to ε–Co in the respective structure. The phase content is not an absolute measure; it may change during the tensile test via strain-induced phase transformation and the ε–Co fraction can increase [12]. The precise influence of this effect needs to be studied further.

The divergences observed in AB conditions are possibly due to varying irradiation in the printing or manufacturing systems. In the heat-treated condition, the differences observed are related to the partial recrystallization that occurred at 800°C in comparison to the full recrystallization at 1150°C followed by furnace cooling, allowing thermodynamic equilibrium conditions. Apart from the HV values, $E, R_{P0.2}, A_t$ and R_m are higher in Co-Cr-W than in Co-Cr-Mo. This simultaneous increase in their respective AB conditions could be an indication that the C-formed curves of the TTT-diagram (Fig. 11) are moved to lower times for the Co-Cr-W alloy. Applying the annealing heat-treatment, E and A_t (except for $\Phi = 90°$) increased, whilst $R_{P0.2}, R_m$ and HV of Co-Cr-W decreased.

Concerning the standards requirements for Type 5 dental alloys, both alloys can be considered suitable for clinical use in their heat-treatment condition. Although AB Co-Cr-W also fulfills these requirements, a heat-treatment is highly recommended, not only to minimize possible distortions from residual stress, but the process also enhances the ductility and stiffness of the material. To guarantee the integrity of the built parts it is recommended that heat-treatment be performed on built parts whilst they are firmly attached to the support structure on the substrate

plate. E and R_m values provided by Co-Cr-W manufacturer is somewhat comparable to ours. A_t values at 0º and 90º in this study are higher than those of the manufacturer whereas our $R_{P0.2}$ values lower. The higher and arbitrary R_m values for Co-Cr-Mo alloy may be due to the increased surface roughness of the specimens, or the possible sub-surface porosity acting as crack initiation [9]. However, these prospective 'inhibitors' were absent in the machined Co-Cr-W specimens with documented studies suggesting the machining process result in improved mechanical properties by enhancing R_m by 5-10% and E up to 10% [39-41].

4.3   Hardness

In our study, we observed minor deviations between micro-hardness (HV5) and macro-hardness (HV20). However, data from the micro-hardness tests (HV5) might be prone to fluctuations due to limited indentation depth (approximately 20 μm at 380 HV5), which is lower than a single layer (~30 μm) and thus, may not be a conclusive measure (**Fig. 13**). For comparison, the indentation depth for 380 HV20 is approximately 40 μm. The hardness tests did not reveal any significant fluctuations regarding the sample orientation. In addition, both alloys exhibited similar HVs in their AB conditions, despite the differences in their $R_{P0.2}$, and R_m values. In their respective HT conditions, HV values differ (~ 435 HV for Co-Cr-Mo and ~ 360 HV for Co-Cr-W), but with comparable R_m values. The disparity between HV values and tensile properties is possibly because hardness testing focuses on compressive stresses whereas tensile test produces failure at uniaxial forces. It is documented that the mechanical properties of SLM-produced alloys do differ in regard to tensile versus compressive loading [42]. Moreover, it is known that the conclusion from hardness to tensile strength is problematic for selective laser melted metal [10].
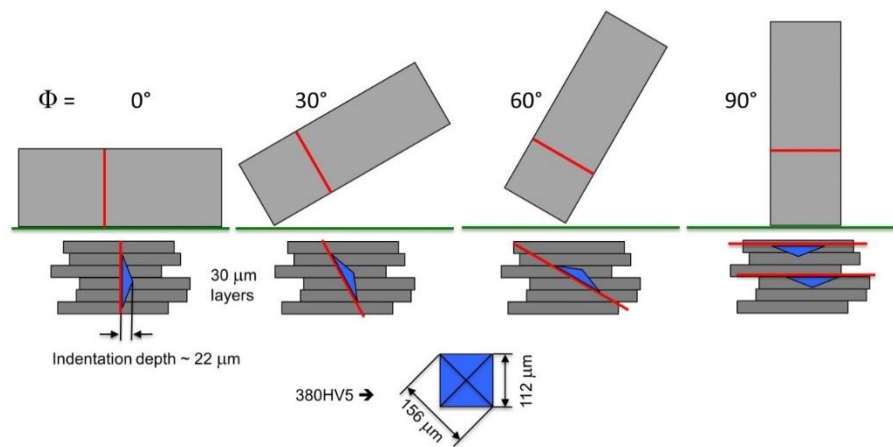
Figure 13. Indentation depth versus layer thickness

5   Conclusion

In this study, we assessed the clinical properties of laser-melted Co-Cr-Mo and Co-Cr-W alloys in as-built and heat-treated conditions. The anisotropy observed in the alloys primarily influenced ductility in addition to minor fluctuations in tensile strength and Young's modulus. In as-built condition, the alloys displayed reduced Young modulus, hence, required heat-treatment to meet clinical requirements set out in the standards. Similarly, heat-treatment is recommended if the desired ductility and isotropic characteristics are to be guaranteed. Although the study confirms the capacity of the SLM systems to produce consistent parts under controlled manufacturing parameters, further microstructure analysis could shed light on phase contents and their alteration via the applied heat treatments.

6   Acknowledgement

7   References

[1] E. Haynes, Metal Alloy, in: U.S.P. Office (Ed.) United States of America, 1907.

[2] A.K. Mishra, M.A. Hamby, W.B. Kaiser, Metallurgy, Microstructure, Chemistry and Mechanical Properties of a New Grade of Cobalt-Chromium Alloy Before and After Porous-

Coating, in: J.A. Disegi, R.L. Kennedy, R. Pilliar (Eds.), Cobalt-Base Alloys for Biomedical Applications, ASTM, West Conshohocken, PA, 1999.

[3] R. Van Noort, Introduction to Dental Materials, 4 ed., Elsevier, Sydney, 2013.

[4] F. Alifui-Segbaya, P. Foley, R.J. Williams, The corrosive effects of artificial saliva on cast and rapid manufacture-produced cobalt chromium alloys, Rapid Prototyping Journal 19(2) (2013) 95-99.

[5] F. Alifui-Segbaya, R.J. Williams, R. George, Additive Manufacturing: A Novel Method for Fabricating Cobalt-Chromium Removable Partial Denture Frameworks, Eur J Prosthodont Restor Dent 25(2) (2017) 73-78.

[6] F. Alifui-Segbaya, J. Evans, D. Eggbeer, R. George, Clinical Relevance of Laser-Sintered Co-Cr Alloys for Prosthodontic Treatments: A Review, Proceedings of the 1st International Conference on Progress in Additive Manufacturing (2014) 115-120.

[7] Food and Drug Administration, Technical Considerations for Additive Manufactured Devices:Draft Guidance for Industry and Food and Drug Administration Staff, 2016.

[8] L. Hitzler, J. Hirsch, B. Heine, M. Merkel, W. Hall, A. Öchsner, On the Anisotropic Mechanical Properties of Selective Laser Melted Stainless Steel, Materials 10(10) (2017) 1136.

[9] L. Hitzler, C. Janousch, J. Schanz, M. Merkel, B. Heine, F. Mack, W. Hall, A. Öchsner, Direction and location dependency of selective laser melted AlSi10Mg specimens, J. Mater. Process. Technol. 243 (2017) 48-61.

[10] L. Hitzler, M. Merkel, W. Hall, A. Öchsner, A Review of Metal Fabricated with Laser- and Powder-Bed Based Additive Manufacturing Techniques: Process, Nomenclature, Materials, Achievable Properties, and its Utilization in the Medical Sector, Adv. Eng. Mater. 20(5) (2018) 1700658.

[11] S. Yager, J. Ma, H. Ozcan, H.I. Kilinc, A.H. Elwany, I. Karaman, Mechanical properties and microstructure of removable partial denture clasps manufactured using selective laser melting, Additive Manufacturing 8 (2015) 117-123.

[12] A. Takaichi, Suyalatu, T. Nakamoto, N. Joko, N. Nomura, Y. Tsutsumi, S. Migita, H. Doi, S. Kurosu, A. Chiba, N. Wakabayashi, Y. Igarashi, T. Hanawa, Microstructures and mechanical properties of Co-29Cr-6Mo alloy fabricated by selective laser melting process for dental applications, J. Mech. Behav. Biomed. Mater. 21 (2013) 67-76.

[13] F. Alifui-Segbaya, J. Lewis, D. Eggbeer, R.J. Williams, In vitro corrosion analyses of heat treated cobalt-chromium alloys manufactured by direct metal laser sintering, Rapid Prototyping Journal 21(1) (2015) 111-116.

[14] SINT-TECH, ST2724G - Technical data: type 5 CoCrMo dental alloy, Riom, France.

[15] Concept-Laser, Technical data in line with DIN EN ISO 9693 / DIN EN ISO 22674 after recommended heat treatment, 2017. https://www.concept-laser.de/fileadmin//user_upload/Datasheet_remanium_star_CL.pdf. (Accessed 22 March 2018).

[16] British Standards Institution, BS EN ISO 22674 - Dentistry: Metallic materials for fixed and removable restorations and appliances, London, United Kingdom, 2016.

[17] 3D Systems, ProX DMP 200, 2018. https://au.3dsystems.com/3d-printers/prox-dmp-200. (Accessed 30 March 2018).

[18] Concept Laser GmbH, Remanium star CL powered by Dentaurum, 2017. https://www.concept-laser.de/fileadmin//user_upload/Datasheet_remanium_star_CL.pdf. (Accessed 30 March 2018).

[19] International Organization for Standardization, ISO 22674:2016: Dentistry - Metallic materials for fixed and removable restorations and appliances, International Organization for Standardization, Geneva, 2016.

[20] Deutsches Institut fuer Normung e.V., DIN EN ISO 6892-1, Metallic Materials—Tensile Testing—Part 1: Method of Test at Room Temperature, Beuth Verlag, Berlin, Germany, 2016.

[21] Deutsches Institut fuer Normung e.V., DIN EN ISO 6507-2, Metallic Materials—Vickers Hardness Test—Part 2: Verification and Calibration of Testing Machines, Beuth Verlag, Berlin, Germany, 2016.

[22] A.B. Spierings, M. Schneider, R. Eggenberger, Comparison of density measurement techniques for additive manufactured metallic parts, Rapid Prototyping J. 17(5) (2011) 380-386.

[23] H. Wulfes, Precision Milling and Partial Denture Constructions, Academia Dental International School BEGO Germany, Bego, 2004.

[24] J.C. Wataha, Alloys for prosthodontic restorations, Journal of Prosthetic Dentistry 87(4) (2002) 351-363.

[25] 3D Systems, CoCrMo alloy for ProX™ 100, 200 and 300 Direct Metal Printers, 2015. https://www.3dsystems.hu/content/pdf/cocrmo_alloy_us_0615_press.pdf. (Accessed 22 March 2018).

[26] S. Leuders, M. Thöne, A. Riemer, T. Niendorf, T. Tröster, H.A. Richard, H.J. Maier, On the mechanical behaviour of titanium alloy TiAl6V4 manufactured by selective laser melting: Fatigue resistance and crack growth performance, Int. J. Fatigue 48 (2013) 300-307.

[27] T. Vilaro, C. Colin, J.D. Bartout, As-Fabricated and Heat-Treated Microstructures of the Ti-6Al-4V Alloy Processed by Selective Laser Melting, Metall. Mater. Trans. A 42A(10) (2011) 3190-3199.

[28] S.P. Faure, L. Mercier, P. Didier, R. Roux, J.F. Coulon, S. Garel, J. Trenit, H. Buard, F. Razan, Laser sintering process analysis: Application to chromium-cobalt alloys for dental prosthesis production, ASME 2012 11th Biennial Conference on Engineering Systems Design and Analysis, ESDA 2012, Nantes, 2012, pp. 9-15.

[29] L. Hitzler, P. Williams, M. Merkel, W. Hall, A. Öchsner, Correlation between the energy input and the microstructure of additively manufactured cobalt-chromium, Defect Diffus. Forum 379 (2017) 157-165.

[30] A. Öchsner, Continuum Damage and Fracture Mechanics, Springer, Singapore, 2016.

[31] L. Hitzler, C. Janousch, J. Schanz, M. Merkel, F. Mack, A. Öchsner, Non-destructive evaluation of AlSi10Mg prismatic samples generated by Selective Laser Melting: Influence of manufacturing conditions, Mat.-wiss. u. Werkstofftech. 47(5-6) (2016) 564-581.

[32] J. Schanz, M. Hofele, S. Ruck, T. Schubert, L. Hitzler, G. Schneider, M. Merkel, H. Riegel, Metallurgical Investigations of Laser Remelted Additively Manufactured AlSi10Mg Parts, Mat.-wiss. u. Werkstofftech. 48(5) (2017) 463-476.

[33] P.B. Hirsch, A. Howie, R. Nicholson, D.W. Pashley, M.J. Whelan, Electron microscopy of thin crystals, Butterworth and Co. Publishers Ltd., London, United Kingdom, 1965/1977.

[34] Y. Kajima, A. Takaichi, N. Kittikundecha, T. Nakamoto, T. Kimura, N. Nomura, A. Kawasaki, T. Hanawa, H. Takahashi, N. Wakabayashi, Effect of heat-treatment temperature on microstructures and mechanical properties of Co–Cr–Mo alloys fabricated by selective laser melting, Mater. Sci. Eng., A 726 (2018) 21-31.

[35] P. Huang, H.F. López, Athermal ε-martensite in a Co–Cr–Mo alloy: grain size effects, Mater. Lett. 39(4) (1999) 249-253.

[36] C.H. Savage, Heat-treatment of cobalt base alloys and products, in: U.S.P. Office (Ed.) 1946, pp. 1-4.

[37] R. Turrubiates-Estrada, A. Salinas-Rodriguez, H.F. Lopez, FCC to HCP transformation kinetics in a Co–27Cr–5Mo–0.23C alloy, J Mater Sci 46(1) (2011) 254-262.

[38] K.C. Li, D.J. Prior, J.N. Waddell, M.V. Swain, Microstructure, phase content, and thermal stability of a cast Co–Cr dental alloy after porcelain sintering cycles using electron backscatter diffraction, J. Mater. Res. 30(14) (2015) 2188-2196.

[39] D. Zhang, Entwicklung des Selective Laser Melting (SLM) für Aluminumwerkstoffe, Fakultät für Maschinenwesen, RWTH Aachen, Germany, 2004, p. 107.

[40] J. Sehrt, G. Witt, Auswirkung des anisotropen Gefüges strahlgeschmolzener Bauteile auf mechanische Eigenschaftswerte, RTejournal, Forum für Rapid Technologie, Duisburg, Germany, 2009.

[41] J.T. Sehrt, Möglichkeiten und Grenzen bei der generativen Herstellung metallischer Bauteile durch das Strahlschmelzverfahren, Maschinenbau und Verfahrenstechnik, University Duisburg-Essen, Germany, 2010.

[42] L. Hitzler, N. Schoch, B. Heine, M. Merkel, W. Hall, A. Öchsner, Compressive behaviour of additively manufactured AlSi10Mg, Mat.-wiss. u. Werkstofftech. 49(5) (2018) 683-688.